ELSEVIER

Journal of Neuroscience Methods 170 (2008) 262–276

JOURNAL OF NEUROSCIENCE METHODS

www.elsevier.com/locate/jneumeth

Immortalization and characterization of lineage-restricted neuronal progenitor cells derived from the porcine olfactory bulb

A. Ulrike Uebing-Czipura [a], Harry D. Dawson [b], Gail Scherba [a,*]

[a] *Department of Pathobiology, College of Veterinary Medicine, University of Illinois at Urbana-Champaign, 2001 South Lincoln Avenue, Urbana, IL 61802, USA*

[b] *Beltsville Human Nutrition Research Center, USDA, Beltsville, MD 20705, USA*

Received 14 February 2007; received in revised form 27 December 2007; accepted 23 January 2008

Abstract

Crucial aspects in the development of *in vitro* neuropathogenic disease model systems are the identification, characterization and continuous mitotic expansion of cultured neuronal cells. To facilitate long-term cultivation, we immortalized porcine olfactory neuronally restricted progenitor cells by genomic insertion of a cDNA encoding the catalytic subunit of the human telomerase reverse transcriptase (hTERT) yielding a stable neuroblast subclone (OBGF400). The altered cells exhibited progenitor-cell-like morphology and mitotic competency based on sustained subpassaging, prevalence in the cell cycle G0/G1 phase and an overall lack of cellular senescence as compared to primary cultures. An OBGF400 neuronal phenotype was indicated by the recognition of a transfected neuronal progenitor-cell-specific tubulin-α1 gene promoter, intracellular presence of early neuronal markers (TuJ1, neuregulin-1, doublecortin and SOX2) and enhanced expression of neuronal- and progenitor lineage-active genes (MAP2, nestin, ENO and Syn1) compared to that of porcine epithelial cells. These OBGF400 neuroblasts are likely dependent on telomerase to prevent terminal differentiation as subcultures with a predominance of neuronally differentiated members had less enzymatic activity. Based on its susceptibility to a porcine alphaherpesvirus infection, this novel neuroblast cell line may be useful for exploring neuronal cell–pathogen interactions *in vitro*.

Keywords: Olfactory bulb; Porcine neuroblasts; Porcine neuronal progenitor cells; Neural transcriptome analysis; hTERT; Alphaherpesvirus

1. Introduction

Biomedical research benefits from the use of natural host–pathogen systems, a situation inherently limited with respect to humans, thereby necessitating animal models. In this regard, swine fulfill the need for a suitable alternative that accurately and precisely emulates many aspects of human structure and physiology. For instance, these animals are similar to humans in terms of organ size, digestive physiology, pulmonary and coronary vasculature, social behaviors, dietary habits and propensity to obesity (reviewed in Tumbleson and Schook, 1996). Their consequential use for medical studies has provided significant advances even to the field of neurology, such as in the understanding of the neurological dysfunctions of Alzheimer's (Smith et al., 1999) and Parkinson's (Mikkelsen et al., 1999) disorders. Furthermore, infectious disease investigations have been advanced most effectively by the direct use of naturally occurring host–pathogen systems. As viral disease outcomes are dependent on interactions of the pathogen with the intracellular macromolecular environment and its surrounding milieu, the pig is an excellent host for studying disturbances of host–viral equilibria that create circumstances conducive for the emergence of lytic and latent viral infections in the nervous system. In this regard, pseudorabies virus (PrV), a natural pathogen of pigs, offers an attractive yet underutilized *in vivo* and *in vitro* system for the direct study of viral infections in the context of the natural host (Scherba and Zuckermann, 1996). Clearly, the development of a suitable *in vitro* neuronal model system will ultimately facilitate the exploration of the multifaceted viral–cell interactions during viral neurotropic pathogenesis. The gained understandings may be relevant to evaluating the impact of other neurotropic viruses on their hosts and applicable to *in vivo* situations. Interestingly, thus far *in vitro* porcine neural cell lines suitable for such model systems are not available due in large part to the low frequency of tumor formation in the porcine central nervous system; an intriguing situation in and of itself. Accord-

* Corresponding author. Tel.: +1 217 244 0929; fax: +1 217 244 7421.
E-mail address: scherba@uiuc.edu (G. Scherba).

0165-0270/$ – see front matter © 2008 Elsevier B.V. All rights reserved.
doi:10.1016/j.jneumeth.2008.01.028

ingly, current *in vitro* models must utilize primary porcine neural cultures, and thus would benefit from the ability to propagate neuronal cells for extended periods of time, an intricate endeavor at best. A major obstacle to this long-term cultivation has been the limited capacity of neuronally restricted progenitor cells for mitotic expansion (Kirschenbaum et al., 1994; Reynolds and Weiss, 1992; Roy et al., 2004).

The loss of mitotic capacity during subpassaging of primary cell cultures can be attributed in some measure to decreased telomerase activity and concomitant shortening of the 3′ ends of the telomeres, a process known to trigger cell crisis through chromosomal fusion and mitotic degradation (Counter et al., 1992). In contrast to primary cells, immortalized cells undergo continuous division, a process enabled by telomerase activity that maintains the length of chromosomal telomeres. Generally, somatic cells exhibit little if any telomerase gene expression (Kilian et al., 1997), whereas multipotent stem cells sustain high telomerase activity and retain their self-renewal potency. In human progenitor cells, such enzymatic activity is typically reduced by the 16th week of gestation or during early subpassaging of cultured cells (Ulaner and Giudice, 1997; Wright et al., 1996). Interestingly, this diminution is partially the result of transcriptional silencing of the catalytic subunit of the telomerase reverse transcriptase (TERT). Thus compensatory ectopic expression of TERT prevents telomere shortening thereby enabling the generation of stable and non-oncogenic cell lines (Counter et al., 1992). Pertinent to our research interests, a recent study by Roy et al. (2004) observed that ectopically induced over-expression of human TERT (hTERT) in neuronal-restricted progenitor cells derived from the human fetal spinal cord significantly extended their life span without compromising responses to mitogenic factors or altering phenotypic characteristics. Moreover, the cells retained karyotype normalcy during serial passaging.

In anticipation of establishing a stable porcine neuronal cell line, the olfactory bulb (OB) should be considered as it is a superior source for the identification and isolation of neuronal lineage-restricted progenitor cells. The OB undergoes neurogenesis even during adulthood and contains multi-lineage as well as lineage-restricted neural progenitors (Liu and Martin, 2003). As a direct extension of the anterior subventricular zone (SVZ) of the lateral ventricle and the rostral migratory stream (RMS), the OB region is the final destination of tangentially migrating neuroblasts. Despite exhibiting biological properties associated with differentiated neurons, these cells maintain their mitotic competence until they reach the more peripheral layers of the OB (Coscun and Luskin, 2002; Lois and Alvarez-Buylla, 1994).

Here we report the extended mitotic competency of such porcine olfactory neuronal progenitor cells after the insertion of a cDNA encoding the catalytic subunit of hTERT into their genomes. This transduced cell line has been stably maintained throughout approximately 100 subpassages with consistent hTERT transcription and activity levels. Moreover, the expression of the tumor suppressor gene p53 and the proto-oncogene c-myc also was found to be unaltered. This neuroblast cell line was phenotypically characterized at the levels of translation by using immunocytochemistry and transcription by utilizing a porcine-specific real-time (r) RT-PCR array. Additionally, to test the suitability of this novel cell line for studies on alphaherpesviruses, their permissiveness to viral infection was determined by monitoring PrV replication and latency-associated transcript (LAT) levels in the immortalized OB neuroblasts. Hence, our approach denotes valuable methodologies for surmounting replicative cellular senescence of committed neuronal progenitor cells and additionally provides comprehensive information on porcine neural gene expression through utilization of a porcine-specific real-time array for a robust transcriptional analysis to characterize this new *in vitro* neuronal cell system.

2. Materials and methods

2.1. Establishment of primary porcine olfactory bulb cell cultures

Olfactory bulbs from 1-day-old pigs were removed and transferred into ice-cold PIPES (piperazine-*N*,*N*′-bis[2-ethanesulfonic acid]) solution (120 mM NaCl, 5 mM KCl, 25 mM glucose, 200 μM glutamine, 20 mM PIPES pH 6.4, 100 U/ml penicillin and 0.1 mg/ml streptomycin) (Sigma, St. Louis, MO). Tissues were minced and dissociated in PIPES solution containing 3 mg/ml collagenase A (Sigma) for 45 min at 37 °C with gentle tituration every 15 min. Following complete dissociation, the cell suspensions were applied to a 40-μm cell strainer (Becton-Dickinson, San Jose, CA) and subsequently centrifuged at 400 × *g* and 4 °C for 10 min. The pellets were then resuspended through gentle pipetting in growth medium consisting of Dulbecco's modified Eagle medium (DMEM)/F12/HAM (Sigma) supplemented with 10% bovine calf serum (Sigma), 100 U/ml penicillin, 0.1 mg/ml streptomycin and 0.05 mg/ml gentamicin (Sigma). Approximately 2×10^6 cells/ml were plated into poly-D-lysine precoated 6-well tissue culture dishes (Midwest Scientific, St. Louis, MO) and incubated at 37 °C in 5% CO_2 for 18 h. Medium was then aspirated to remove non-adherent cells and replaced with fresh growth medium every 48–72 h. After at least 10–12 days in culture, the cells were trypsinized, plated by limiting dilution to select for mitotically competent, adherent cells and incubated as described above for at least 4–5 days prior to the immortalization procedure. All resultant cultures displayed similar morphology.

2.2. Cellular immortalization

The established primary heterogeneous porcine OB cultures were infected with a murine leukemia virus-pseudotyped amphotrophic retrovirus designed to express hTERT. Production of the amphotrophic retrovirus was achieved through co-transfection of an hTERT cDNA-containing pBabe-Neo vector (p0196) and a pCL-10A1 (p0467) packaging construct (both generous gifts from Dr. C. Counter, Duke University) into 293TS cells as previously described (Counter et al., 1998). Briefly, 3 μg of each vector and 12 μl Fugene-6 (Roche, Indianapolis, IN) were mixed in 200 μl of serum-free minimum essential medium (Sigma) and incubated at 25 °C for 15 min. The transfection mix-

ture was then applied directly to a 60% confluent 293TS cell monolayer and incubated at 37 °C in 5% CO_2. This procedure was repeated 24 h after the first transfection and fresh growth medium replaced the transfection mixture 12 h later. After an additional 36 h of incubation, the released amphotrophic retrovirus was harvested in the culture media and filtered through a 0.45-μm Acrodisc HT tufftyn membrane (Pall Corp., Ann Arbor, MI). The virus-containing filtrate, supplemented with 4 μg/ml polybrene (Sigma), was then applied to the primary olfactory neural cell cultures twice at 12 h intervals during incubation at 37 °C in 5% CO_2. For comparative purposes, cultures of mock-infected primary OB cells (L-OB hTERT$^-$) were continuously maintained in growth medium.

A neomycin-resistance gene, located downstream of the hTERT expression construct, was utilized for the selection of transduced, and presumably, immortalized cells. Starting 48 h after the second infection, the primary OB cultures were maintained for at least 10 days in growth medium containing 400 μg/ml G418 (Sigma, a concentration previously determined to induce 100% mortality within 3 days of primary OB cultured cells, L-OB hTERT$^-$). Following the selection process, the very few surviving and replicating cells (less than 1% of the initial population) were allowed to propagate without selection (as directed by the immortalization protocol) for at least 4 weeks prior to the first subpassage. Once the monolayers were 60% confluent, the cells were subjected to a series of limiting dilutions to establish a replicating homogenous subclone, designated OBGF400.

To confirm stable and persistent ectopic hTERT overexpression over time, cultures that have undergone at least 100 subpassages (late) were again subjected to G418 exposure (400 μg/ml) as described above. Non-hTERT-transduced, transformed cultures of Crandell-Rees feline kidney (CRFK) and porcine kidney (PK15) cell lines were used as controls.

For the analysis of their replicative capacity, OBGF400 cells from early (<20 subpassages) and late cultures were seeded at a density of 2×10^3 cells in 6-well tissue culture plates (Midwest Scientific) and were maintained in growth medium. Growth rates were subsequently analyzed by counting the total cell number every other day during a 6-day period with day 0 representing the day of plating. For each subpassage phase, the cells in three independent wells were counted using a hemocytometer and the totals were averaged for each time point.

2.3. Telomerase repeat amplification protocol (TRAP) assay

To assess telomerase activity in the immortalized (early, ≤20 subpassages) versus primary (L-OB hTERT$^-$) OB cultures as well as in late subpassage OBGF400 cultures that had or had not undergone re-exposure to the neomycin analog, G418, a TRAP assay was conducted using the TRAPeze Detection Kit (Chemicon International, Inc., Temecula, CA). Primary cell cultures were used prior to mitotic deceleration or phenotypic degradation. In addition, hTERT expression levels were determined for early OBGF400 cell cultures exhibiting various degrees of neuronal maturation. The criteria for the assessment of morphological change indicative of neuronal maturation (terminal differentiation) were the presence of bipolar or multipolar cell processes and a more prominently defined yet smaller cell body. Cellular lysates from OBGF400 and L-OB hTERT$^-$ cultures (10^5 cells per sample) and a telomerase positive control cell extract (kit reagent) were prepared per manufacturer's recommendation. As a contamination control, aliquots of each sample were heat-treated at 85 °C for at least 10 min to inactivate endogenous telomerase prior to being assayed.

Telomerase substrate (TS) primers (kit reagent) were end-labeled with (γ^{32}P) dATP using T4 polynucleotide kinase (Invitrogen, San Diego, CA) during a 20-min incubation at 37 °C and the reaction was subsequently terminated at 85 °C for 5 min. For telomerase extension, the labeled TS primers and TS template (kit reagent) were then incubated at 30 °C for 30 min with each cellular lysate, their heat-treated match, the telomerase positive control cell extract, a TSR8 quantification control (kit reagent) and a buffer-only control (used to assess primer dimerization). When active telomerase was present, telomeric repeats were added to the 3′ end of the oligonucleotide TS template, generating a ladder of labeled products in 6-base increments, starting at 50 nucleotides. These products then were amplified in a hot-start PCR protocol for a total of 30 cycles of 94 °C for 30 s and 59 °C for 30 s. To estimate the total product generated (TPG) for each sample, the amplicons were separated during vertical electrophoresis in a non-denaturing 12% polyacrylamide gel (Jule, Inc., Milford, CT) and subsequently visualized by using autoradiography. Autoradiogram densitometric analysis for the quantification of the telomerase activity was performed using a computer-linked scanner (UMAX PowerLook 2100XL scanner with Magic Scan v4.5, UMAX Technologies, Fremont, CA) and analysis software (Discovery Quantity One, Bio-Rad Laboratories, Inc., Hercules, CA). The area of each TRAP product was measured three times and the respective sums were averaged to provide the total area of synthesized TRAP products in each sample. These values were used to calculate the TPG as recommended by the manufacturer.

2.4. rRT-PCR for hTERT, c-myc and p53 gene expression in OBGF400 cells

The levels of hTERT, c-myc and p53 mRNA were examined in OBGF400 cultures of early and late (with or without G418 re-exposure) subpassage time points, and from early cultures containing cells depicting various degrees of cellular differentiation based on morphological change. Total RNA was extracted by using the RNeasy Mini Kit (Qiagen, Valencia, CA) and then DNase-treated at 37 °C for 20 min using TURBO DNase (Ambion, Austin, TX). Subsequently, each sample was purified and concentrated with RNeasy Clean-Up Columns (Qiagen). Concentrations and purity of total RNA preparations were determined by using a Nanodrop™ spectrophotometer (Nanodrop Technologies, Wilmington, DE). Reverse transcription reactions were performed with 1 μg of total RNA and oligo-dT primers using the First-Strand cDNA Synthesis System (Invitrogen).

The levels of hTERT gene expression were established using Assays-on-Demand primers and probe (Applied Biosys-

Table 1
Real-time RT-PCR primers and probes for the detection of porcine transcripts

Gene ID	Description	Primer sequence	Probe sequence (5′FAM/3′BHQ)	Size (bp)
CNPase	2′,3′-Cyclic nucleotide 3′-phosphodiesterase	F: 5′-TTGGCTGGTTCCTGTCCAG-3′; R: 5′-GCCAAAGTGTCGCAGCTCTT-3′	CCTCCGCAAAGCCGGCCA	112
ENO	Neuron-specific enolase	F: 5′-GGAGAGACTGAGGACACGTTCAT-3′; R: 5′-TGGTTGTACTTAGCCAGACGTTCA-3′	CCAGATCAAGACTGGTGCCCCGTG	106
GFAP	Glial fibrillary acidic protein	F: 5′-CAGAGCCTCAAGGACGAGATG-3′; R: 5′-AGGAATGGTGATGCGGTTCT-3′	CATCGAGATCGCCACCTACAGGAAGC	134
ITGAM	Integrin alpha M (CD11b)	F: 5′-CGAAGAGTCTACGGCCTTGAAG-3′; R: 5′-GGTCACGTTGGCCTTGAGAA-3	AGCATAAACCACCCCATCTTCCCGGA	147
L32	Ribosomal protein	F: 5′-TGGAAGAGACGTTGTGAGCAA-3′; R: 5′-CGGAAGTTTCTGGTACACAATGTAA-3′	ATTTGTTGCACATTAGCAGCACTTCAAGCTC	93
LAT	PrV latency-associated transcript	F: 5′-CTCCAGGCCCAGACAAAAT-3′; R: 5′-AGACTCCCTCAGCCATAGAAGAC-3′	TCCGTCTCTCCCGCCCGGT	84
MAP2	Microtubule-associated protein 2	F: 5′-TGCCGGAAGAGTCAAAGATGA-3′; R: 5′-CTGATCAAACTCCTTACTCAGTCCTG-3′	AGTGCCGAGAAAGAAGCAGCCCCAC	93
MAP1B	Microtubule-associated protein 1B	F: 5′-GCATTCTCTTGCTATGGACTTCAG-3′; R: 5′-TTGGCCCATTTTCAGTGATG-3′	CGACAGTCTCCAGATCACCCTACAGTGG	88
MOG	Myelin oligodendrocyte glycoprotein	F: 5′-TCAGGATCCGGCATGTAAGG-3′; R: 5′-AAGGGATCTTCCACTTTCAATTCC-3′	CCTGCTTCTTCCGAGATCATTCTTACCAAGAG	108
MYC	Proto-oncogene	F: 5′-CACGAGGAGACACCACCCAC-3′; R: 5′-AAACAACATCAATTTCTTCCTCATCTT-3′	TGTTCCTCCTCAGAGTCGCTGCTGGT	76
Nestin	Progenitor-specific nestin	F: 5′-CCTGGGCCAGAGCCAGTT-3′; R: 5′-CTCCCCTGAGGACCAGGAAT-3′	TCCATCTCCCTCTCTCTGAGTGAACGGC	69
NTRK	Tyrosine kinase A (TrkA)	F: 5′-GAGCTGAGGAACCTCACCATTG-3′; R: 5′-AGGAGTGAAATGGAAAGCATCTG-3′	CGCCACGAAACGGAGACCACTCTTC	71
TP53	Tumor suppressor protein 53	F: 5′-TTCTGGAACAGCCAAGTCTGTAA-3′; R: 5′-GGCAGGTCTTGGCCAGCT-3′	TGCACGTACTCCCCTGCCCTCAA	80
S100	Calcium-binding protein	F: 5′-TTTCCCACTTCCTGGAGGAAA-3′; R: 5′-CCATGAATTCCTGGAAGTCACA-3′	CCATGACTTTGTCCACGACCTCCTGCT	104
Syn1	Synapsin 1	F: 5′-CGCCGCAGCCATGAAC-3′; R: 5′-TGTACCCATTTGGCAGATTGG-3′	CGCCGCCTGTCGGACAGCA	93

tems, Foster City, CA; Assay No. Hs00162669_m1) and the TaqMan™ Universal PCR Master Mix (Applied Biosystems) following the manufacturer's recommendations. Comparison of hTERT, c-myc and p53 transcriptional levels in cells from early and late subpassages was performed utilizing three independent cultures for each time point. In addition, the hTERT gene expression in OBGF400 cultures containing cells in various degrees of neuronal maturation was assessed in a total of six cultures derived from individual subpassages, with each reaction performed as a technical triplicate.

rRT-PCR was conducted using the TaqMan™ Universal PCR Master Mix (Applied Biosystems) standard protocol. All primers and probes (Biosource International, Camarillo, CA) were designed based on porcine-specific gene sequences (Table 1). Final primer and FAM(BHQ)-labeled probe concentrations were 900 and 200 nM, respectively. Primer specificity was confirmed using total RNA extracted from the porcine OB tissue. Determination of a PCR efficiency of 100% (±10%) was based on standard curves for each primer/probe set. The C_t values were determined using the autoanalyze feature of the ABI PRISM 7000 Sequence Detection System (Applied Biosystems). Relative gene expression, normalized to L32 ribosomal protein transcript levels, was quantified using the $\Delta\Delta C_t$ method (Livak and Schmittgen, 2001), where $\Delta\Delta C_t = (C_{t\,\mathrm{OBGF400early}} - C_{t\,\mathrm{L32}}) - (C_{t\,\mathrm{OBGF400late}} - C_{t\,\mathrm{L32}})$. The fold change in the target gene was calculated for each sample using the formula: $2^{-\Delta\Delta C_t}$.

2.5. Construction of pCI-tubulin-α1 (Tα1)-green-fluorescent protein (GFP) and pDrive-hβ-actin-GFP expression vectors

A 1.1-kb fragment containing the rat tubulin-α1 promoter and upstream sequence elements was amplified from pTα1:n*lac*Z (kindly provided by Dr. F.D. Miller, University of Toronto). To enable directional insertion, the forward primer TuPro1-For (5′-AGCTAGATCTCTGAATTCCGTATTAGAAGGGATGGC-3′) contained a BglII restriction site at its 5′ end and the reverse primer TuPro1-REV (5′-ATACGCGTAGGAGGTGTTGCTTCTTACAGCG-3′) was designed with a MluI restriction site at its 5′ end. The resultant amplicon was co-digested with BglII and MluI and subsequently ligated into a similarly restricted enhanced green-fluorescent protein (EGFP) expression vector (pCI-GFP) (a gift from Dr. W.M. Schnitzlein, University of Illinois, Urbana-Champaign) to generate the promoter-defined EGFP expression vector, pCI-Tα1-GFP.

A second vector was constructed in which the constitutively active human β-actin promoter was used to regulate EGFP gene expression. In this case, plasmid pEGFP (Clontech, Mountain View, CA) was co-digested with EcoRI and NcoI to release the EGFP ORF. The resultant 704 bp fragment was then ligated into the identically restriction endonuclease-digested pDrive-hβ-actin vector (Invitrogen) to generate pDrive-hβ-actin-GFP.

2.6. Transient transfection of OBGF400 cells

OBGF400 cells from early-subpassaged cultures were pelleted at $900 \times g$ for 10 min and suspended in Cell Line Nucleofector™ Solution V (Amaxa GmbH, Cologne, Germany) at a density of 1×10^6 cells/100 μl from which 100 μl volumes were aliquoted into Nucleofector™ cuvettes. After the addition of 2 μg of either pCI-Tα1-GFP or pDrive-hβ-actin-GFP, the cells were pulsed in the Nucleofector™ device (program T-30). OBGF400 cells similarly pulsed in the absence of vector DNA served as a negative control. Immediately after nucleofection, the OBGF400 cells were mixed with 500 μl of prewarmed growth medium and transferred into 25 cm^2 culture flasks (Midwest Scientific) containing prewarmed growth medium. The cells were incubated at 37 °C and 5% CO_2 until GFP expression was evaluated by using flow cytometry, typically within 48–72 h after transfection, to determine the percentage of neuronally restricted OBGF400 cells that recognized the Tα1 promoter. For this purpose, transfected OBGF400 cells were washed once with sterile PBS prior to being harvested by trypsinization. The cells were centrifuged at $600 \times g$ for 7 min at 25 °C, suspended in 1 ml DMEM/F12/HAM and kept at 4 °C. A total of 3×10^3 cells ($n = 4$) transfected with either expression vector were analyzed for GFP-fluorescent intensity through a 530/540-nm band pass filter as they passed through a laser beam of 488 nm in a LSR II bench top instrument (BD Biosciences, San Jose, CA) at the University of Illinois, Roy J. Carver Biotechnology Center, Flow Cytometry Facility. Nucleofector™-pulsed but non-transfected OBGF400 cells were used to establish the background. Net transfection efficiency was based on the percentage of GFP^+ cells in each transfected population.

2.7. Immunochemical staining of OBGF400 cells

2.7.1. Cells

OBGF400 cells were seeded in Lab-Tek™ II CC2 4-well chamber slides (Nunc, Inc., Wiesbaden, Germany). After the monolayers had reached at least 70% confluency, they were fixed with 4% paraformaldehyde (Ted Pella, Inc., Redding, CA) for at least 30 min at 25 °C. Monolayers containing a significant portion of cells displaying a morphological change indicative of differentiation were also fixed for evaluation. Blocking and permeabilization was conducted for 60 min at 4 °C using a 1:20 dilution of BioFX milk (BioFX Laboratories, Owings Mills, MD) in PBS containing 0.1% Triton-X-100 (Sigma). Subsequently, the cells were washed three times with PBS, then incubated with one of the primary antibodies at 37 °C for at least 60 min. These primary antibodies were diluted in PBS containing 0.1% Triton-X-100 as follows: mouse anti-β-III-tubulin (TuJ1; 1:1000; Chemicon International, Inc.), rabbit anti-neuregulin-1 (Nrg1; 1:100; Abcam, Cambridge, MA), goat anti-doublecortin (DCX; 1:50; Santa Cruz Biotechnologies Inc., Santa Cruz, CA), goat anti-SOX2 (1:50; Santa Cruz Biotechnologies Inc.), mouse anti-Ki-67 (1:50; BD Biosciences, San Jose, CA), mouse anti-glial fibrillary acidic protein (GFAP; 1:500; Chemicon International, Inc.), mouse anti-2′,3′-cyclic nucleotide-3′-phosphodiesterase (CNPase; 1:100; Abcam), mouse anti-A2B5 (1:100; Chemicon) and mouse anti-actin (undiluted, BioGenex, San Ramon, CA). To ensure porcine-specificity of the primary mouse antibodies, normal mouse IgG_1 (1:100; Southern Biotechnologies, Birmingham Alabama) was used as an isotypic control. After three washes with PBS, the cells were incubated for 90 min in the dark at 4 °C with the respective FITC-conjugated secondary antibody (1:200; Jackson ImmunoResearch Laboratories, West Grove, PA) diluted in PBS containing 0.1% Triton-X-100. A secondary antibody-only control was included to assure specificity of these reagents. Following three washes with PBS, the cells were overlaid with mounting media (PBS:glycerol [1:1]) and coverslipped.

2.7.2. OB tissue

To confirm porcine reactivity of the primary antibodies, OB tissue sections were utilized as additional controls. Olfactory bulbs from 1- to 3-day-old pigs were removed, washed once with PBS and immediately mounted in Neg-50 (Richard-Allan Scientific, Kalamazoo, MI), quick-frozen on dry ice and then stored at −80 °C until use. The mounted OBs were cryosectioned at a thickness of 8 μm, and then dried at 37 °C for at least 2 h or at 25 °C overnight. The dried sections were fixed with 4% paraformaldehyde for at least 20 min at 25 °C and then processed as described above for immunocytochemistry. As before, normal mouse IgG- and secondary antibody-only treated tissues were included as negative controls.

2.8. Digital imaging of OBGF400 cells

Microscopic imaging of the immunocytochemistry and immunohistochemistry results was performed using a Spot RT slider CCD camera fitted to a Nikon E600 fluorescent microscope. For images of cultured OBGF400 cells, the camera was fitted to a Nikon Eclipse TS100 inverted microscope. All images were captured and processed using Metamorph 6.0 software (Universal Imaging, Inc., Molecular Devices, Downingtown, PA).

2.9. Cell cycle analysis of OBGF400 cells

A DNA content protocol, as previously published (Ormerod, 1992), was utilized to determine the percentage of cells in the G0/G1 to G2 phases of the cell cycle. Cells were examined following the initial G418 selection procedure or from late subpassage (with or without G418 re-exposure) cultures. For each initial (early) and late subpassage, two independent, nearly 70% confluent monolayers (approximately 5×10^5 cells) were harvested by trypsinization each day during a 3-day period ($n = 6$). The released cells were pelleted by centrifugation and then suspended in 200 μl cold PBS (without Ca^{2+} or Mg^{2+}, Sigma). Four milliliters of ice-cold 70% ethanol was added in a dropwise fashion to the suspended pellets during gently vortexing. The cells then were incubated for 1 h at 4 °C and then stored at −20 °C until analysis. For flow cytometry, the fixed cells were pelleted by centrifugation then suspended in 1 ml of propidium iodide (PI) master mix consisting of PBS (without Ca^{2+}

or Mg^{2+}), 40 μg PI (Sigma) and 0.1 μg RNase A (Worthington Biochemicals, Lakewood, NJ) per sample, gently mixed, and incubated for at least 30 min at 37 °C. Afterwards, the cells were examined by using the LSR II instrument. Fluorescent emissions were detected in a FL3 fluorescence channel with a 695/40-band pass filter. Analysis of the data was performed using the cell cycle modeling software, ModFit LT Version 3 (Verity Software House, Inc., Topsham, ME) in the manual analysis mode. Results for each phase of the cell cycle were independently averaged. Another analysis was performed using the MultiCycle program for the interpretation of abnormal DNA content to enable the detection of aneuploidy.

2.10. Transcriptional analysis of OBGF400 cells

Total RNA was independently isolated from 90% confluent monolayers of early-subpassaged OBGF400 and of PK15 (non-neuronal) cells in three 75 cm^2 flasks (Midwest Scientific) by using the RNeasy Mini Kit (Qiagen) and from approximately 10 to 20 mg of minced OB tissue obtained from 1- to 3-day-old pigs by using the RNeasy Lipid Tissue Kit (Qiagen) following manufacturer's recommendations. Methods for DNase I treatment as well as subsequent RNA purification, RNA concentration determination and cDNA synthesis are described above.

rRT-PCR was conducted for selected genes (Table 1) using the TaqMan™ Universal PCR Master Mix (Applied Biosystems) standard protocol as described above. Relative gene expression, normalized to that of the L32 gene, was quantified using the $\Delta\Delta C_t$ method (Livak and Schmittgen, 2001), where $\Delta\Delta C_t = (C_{t\,OBGF400} - C_{t\,L32}) - (C_{t\,PK15\,or\,OB\text{-}tissue} - C_{t\,L32})$. The fold change in the target gene was calculated for each sample using the formula: $2^{-\Delta\Delta C_t}$.

Three separate RNA preparations (biological replicates) for each cell type were carried through the analysis in duplicate. The results for the biological replicates were averaged prior to calculating fold differences.

2.11. Cellular senescence assay

The Cellular Senescence Detection Kit (Biovision, Mountain View, CA) was used to histochemically detect senescence-associated β-galactosidase (SA-β-Gal) expression. To assess the correlation between β-galactosidase activity and cellular differentiation status in the early cultures, OBGF400 cells were seeded in 24-well plates (Midwest Scientific) at an approximate density of 10^5 cells/ml. Cultures were maintained in growth medium and incubated at 37 °C in 5% CO_2 for at least 6 days. The monolayers were subsequently fixed and stained for the presence of β-galactosidase according to manufacturer's instructions. The cells were microscopically analyzed for SA-β-Gal expression as determined by a blue chromogenic reaction within the cytoplasm. The negative control consisted of rapidly dividing CRFK cells that failed to demonstrate SA-β-Gal staining.

For statistical validation, three replicates (one replicate defined as three individual wells of independently subpassaged cells) were analyzed. Each of the 9 wells was divided into 20 fields resulting in 180 fields containing a total of 2007 cells. The cells in each field were manually counted and matched to one of four categories: presence of SA-β-Gal expression in immature versus mature (terminal differentiation) neuronal cells as delineated above or absence of SA-β-Gal activity in immature versus mature neuronal cells. The total number of cells from the three individual wells comprising a replicate (total of 60 fields) was summed for each category and the average of all three replicates per category was subjected to bivariate tabular analysis using the Chi-square test for population variance.

2.12. Alphaherpesvirus infection of OBGF400 cells

To determine the susceptibility of the OBGF400 cells to the porcine alphaherpesvirus PrV, cells were seeded in Lab-Tek™ II CC2 4-well chamber slides (Nunc, Inc.) at a density of 4×10^5 cells per well and subsequently exposed to PrV-Becker (PrV-Be) expressing green-fluorescent protein (PrV-Be-GFP, kindly provided by L.W. Enquist) at a moi of 1. Sixteen hours later, culture fluids were harvested for subsequent titration of infectious virus. At this time, the cells were fixed in 2% paraformaldehyde at 25 °C for 40 min prior to microscopic analysis of GFP expression as described above for digital imaging. CRFK cells were used for PrV-Be-GFP propagation and titrations. Titers were calculated by using the Reed-Muench method as described elsewhere (Hierholzer and Killington, 1996; Jin and Scherba, 1999).

2.13. Detection of the PrV LAT in virus-infected OBGF400 cells

PrV LAT expression in the late subpassage OBGF400 neuroblast cell line was analyzed at 0, 4, 6 and 8 h post-infection (hpi). Cells were propagated in a total of twelve 75 cm^2 flasks (Midwest Scientific) and triplicate cultures for each time point as well as corresponding mock-infected cultures were used. Approximately 90% confluent cell monolayers were infected with PrV-Be at a moi of 5. Total cellular RNA was harvested at various time points and the subsequent RNA purification, RNA concentration determination as well as cDNA synthesis were performed as described above. rRT-PCR for the LAT was conducted using the TaqMan™ Universal PCR Master Mix (Applied Biosystems) standard protocol. PrV LAT-specific primer and the analogous FAM(BHQ)-labeled probe (Biosource International) were designed based on the NCBI GenBank #NC_006151 complete, annotated PrV genome sequence (Table 1, Klupp et al., 2004); final primer and probe concentrations were at 900 and 200 nM, respectively. The methodology used to determine the C_t values, as well as the consequential relative gene expression quantification and normalization routines using L32 gene expression are as described for the cellular transcriptional analysis.

3. Results

3.1. Immortalization of primary porcine OB cell cultures

Primary heterogeneous cell cultures derived from the OBs of neonatal pigs were established in the absence of anti-mitotic

reagents. Following limiting dilutions, the established primary neural cultures were infected with an amphotrophic retrovirus designed to stably insert an hTERT cDNA into the cellular chromosomes. Matched control cultures were simultaneously mock-infected and maintained under equivalent conditions to the retroviral-infected cells. Successful transduction of the hTERT cDNA into the OB neural cells was based on their neomycin (G418) resistance, whereas all mock-infected cells died during the antibiotic selection process. The hTERT-immortalized cell cultures, which contained very few replicating cells (less than 20) after selection, were propagated and then subjected to limiting-cell dilution to establish a homogenous cell population. One particular subculture (designated OBGF400) displayed progenitor-like (immature) morphology, and thus was chosen for clonal expansion. The L-OB hTERT$^-$ cells (mock-infected and without G418 selection) terminally differentiated and experienced rapid mitotic deceleration after approximately 6 weeks in culture and, hence could not be further maintained under the described conditions. In contrast, the hTERT-transduced counterparts persistently divided in the presence of calf serum.

Individual growth curves for cultures of early (<20 subpassage) and late (at least 100 subpassage) OBGF400 cells were established over a period of 6 days (Fig. 1). Both subpassages had similar growth curves with an approximate doubling time of 4 days indicating consistent growth kinetics unaltered by continuous subpassaging. Moreover, the cells have retained contact inhibition regardless of subpassage level.

Furthermore, the growth characteristics of the OBGF400 cells from late subpassage cultures remained unaffected when exposed again to G418 selection levels of 400 μg/ml. In contrast, the non-hTERT-transduced, transformed cell line controls, CRFK and PK15, did not survive beyond 4 days in culture under selection conditions. This survival indicated that the neomycin-resistance gene, and presumably the hTERT expression cassette, remained stably inserted in a transcriptionally active state in the genomes of the OBGF400 cells despite numerous subpassaging events in the absence of G418. It should be noted that such observed retention is in agreement with the findings from others utilizing this methodology (Dr. C. Counter, Duke University, personal communication).

Cultures of the subpassaged hTERT-immortalized OBGF400 cells (Fig. 2A) almost always contained a few members with

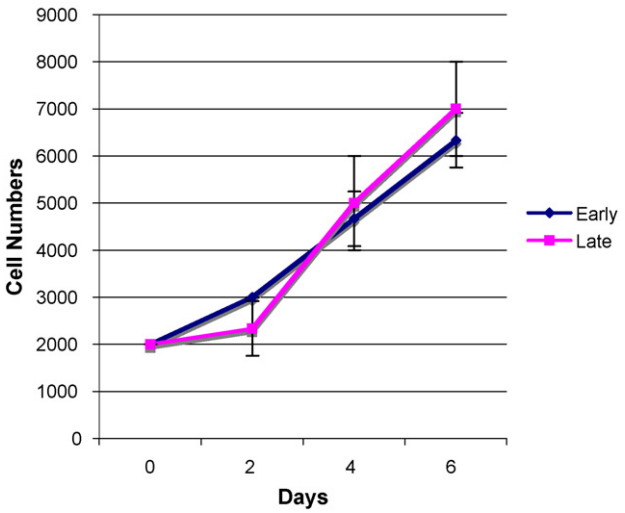

Fig. 1. OBGF400 cell growth kinetics. OBGF400 cells from the early and late subpassages were seeded into 6-well plates on day 0 at a density of 2×10^3 cells per well. The total number of cells within three independent cultures from each subpassage phase were determined at the indicated times and then averaged.

asynchronous morphological changes consistent with terminal differentiation and the consequential loss of phenotypic uniformity (Fig. 2B and C). These presumed, terminally differentiated (mature) OBGF400 cells did not proliferate *in vitro* and their life span failed to exceed 10 days post-differentiation. The degree of morphological change among the different OBGF400 cell cultures and subpassages varied despite equivalent growth and subpassaging conditions, and thus appeared to occur randomly. Overall, only a very few cultures contained a significant proportion of differentiated cells.

3.2. Assessment of telomerase activity in immortalized OBGF400 cells and non-transduced primary OB cells

When the relative net telomerase activities in early-subpassaged hTERT cDNA-transduced OBGF400 cells and L-OB hTERT$^-$ cells were determined by using TRAP assays, the former was always greater despite culture-to-culture variability. In the presented example (Fig. 3A, lanes 1 and 3), the difference was found to be 7.9-fold (142 TPG/10^5 vs. 18 TPG/10^5 cells). Thus, the mitotic competence of the OBGF400 cells positively correlated with enhanced telomerase activ-

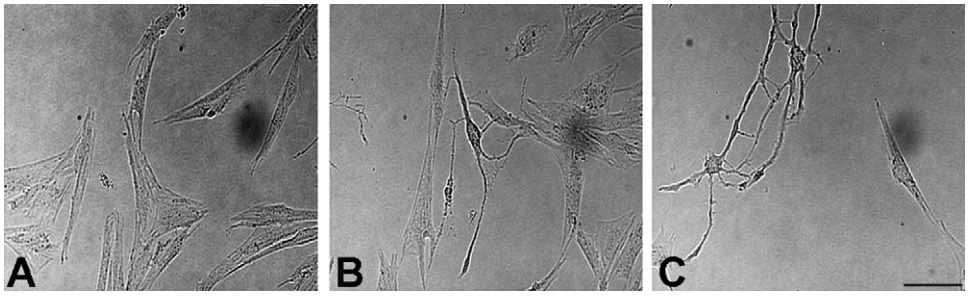

Fig. 2. Morphology of OBGF400 cells. Light microscopic images (20× objective) of cultured OBGF400 cells exhibiting immature morphology (A) and those with progressively mature (B and C) neuronal morphology, which consisted of bipolar to multipolar cell processes, a more prominently defined cell body and significant size reduction. Size marker in panel (C) represents 100 μm.

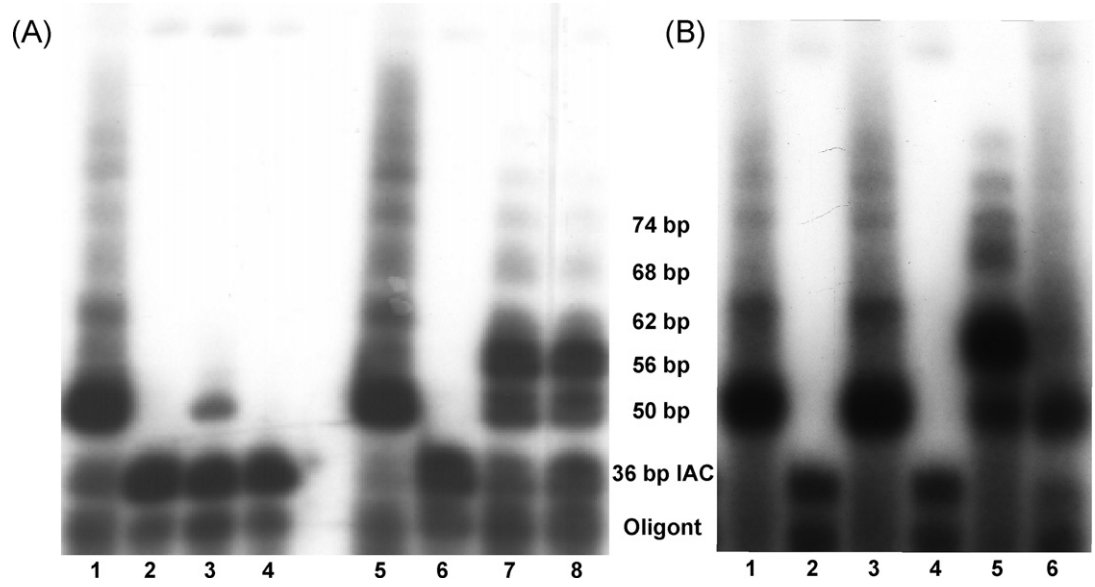

Fig. 3. Assessment of telomerase activity in immortalized and primary OB cell cultures. Cellular lysates were subjected to TRAP assays and the resultant products, separated by non-denaturing 12% polyacrylamide gel electrophoresis, were detected by using autoradiography. (A) Lysates of early-subpassaged OBGF400 (hTERT-immortalized) cells (lane 1), primary L-OB hTERT^{-} cells (lane 3) and their respective heat-inactivated counterparts (lanes 2 and 4). Controls consisted of a telomerase positive extract (lane 5), a primer–dimer PCR contamination control (lane 6) as well as 2 and 1 μl of a telomerase quantification control template, TSR8 (lanes 7 and 8, respectively). (B) Lysates of late subpassages of OBGF400 (hTERT-immortalized) cells with (lane 1) or without (lane 3) G418 re-exposure and their respective heat-inactivated counterparts (lanes 2 and 4). The telomerase positive extract (lane 5) as well as 1 μl of a telomerase quantification control template, TSR8 (lane 6), is shown. The presence of active telomerase is indicated by a ladder of amplicons (TRAP products) with 6-base pair (bp) increments starting at 50 bp. Each reaction also produced a 36 bp internal amplification control (IAC) and contained unincorporated oligonucleotides (oligont).

ity. Continuous subpassaging of the OBGF400 cells in the absence of the selection agent G418 did not negatively influence hTERT expression as 239 TPG/10^5 cells were quantified in late-subpassaged monolayers (Fig. 3B, lane 1). Neither did subsequent re-exposure to G418 for 10 days as the level of telomerase activity was measured at 288 TPG/10^5 cells in the drug-treated monolayers (Fig. 3B, lane 3). Therefore, a stable and persistent ectopic expression of the foreign hTERT cDNA in the OBGF400 cells proceeded in the absence of continuous selective pressure for the maintenance of the co-linked neomycin-resistance gene.

3.3. Assessment of hTERT cDNA, c-myc gene and p53 gene expression in the immortalized OBGF400 cells

To determine whether hTERT transcript levels correlated with the amounts of telomerase activity detected by the TRAP assay in the early- and late-subpassaged OBGF400 cells, relative rRT-PCR was performed. As with the enzymatic activity, there was a slight enhancement in relative hTERT transcript quantities in the late-subpassaged cells before (1.5-fold greater) and after (3.2-fold greater) G418 exposure as compared to the early-subpassaged cells. In addition, the transcriptional levels of the proto-oncogene c-myc and the tumor suppressor p53 gene were ascertained to evaluate the immortalized phenotype of the OBGF400 cell line. In contrast to the hTERT mRNA levels, c-myc and p53 gene expressions were more consistent with relative transcript levels of 1.0- and 1.4-fold, respectively, for the untreated, late-subpassaged cells and 1.4- and 0.83-fold, respectively, for the G418-exposed, late-subpassaged cells. Thus, while the renewal of selective pressure correlated with a slight increase in the amount of hTERT transcripts in OBGF400 cells, neither this precaution nor simply the continuous subpassaging of the cells without selection had an obvious impact on c-myc and p53 gene expression.

3.4. Assessment of neuronal-restricted Tα1 promoter activity in immortalized OBGF400 cells

To verify the predicted neuronal lineage of the OBGF400 cells, they were transfected with pCI-Tα1-GFP and subsequently analyzed for the presence of GFP by using flow cytometry. Whereas the non-transfected cells produced very little GFP (Fig. 4A), and thus were used to set the GFP-positive gate at 1.1% of this population, 36.6% of the tested OBGF400 cells expressed various amounts of GFP (Fig. 4B). Since the Tα1 promoter has been shown to be active only in progenitor cells exclusively destined to be in the neuronal lineage (Gloster et al., 1994; Miller et al., 1987; Wang et al., 2000), its demonstrated transcriptional regulation of the associated GFP gene in the transfected OBGF400 cells supports their designation as neuronal lineage-restricted cells and demonstrated their homogeneous nature.

Since the transfection competency of neuronal cells is usually much less than that of established mammalian epithelial and fibroblastic cell lines, it was not surprising that the overall percentage of successfully transfected OBGF400 cells was less than 50%. However, to determine whether this level of

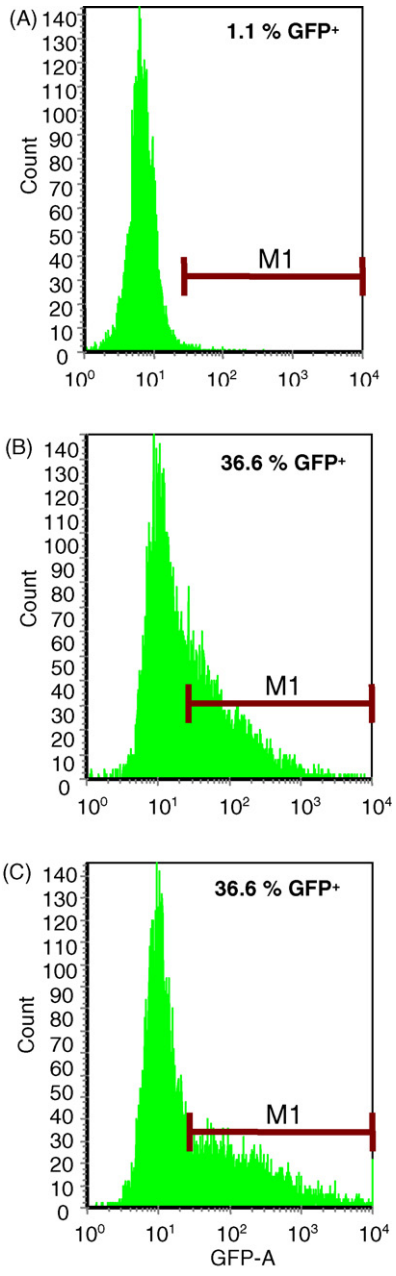

Fig. 4. Assessment of the transfection efficiency of OBGF400 cells and their recognition of the Tα1 gene promoter. Flow cytometry histograms of GFP-fluorescent intensity of mock (A), pCI-Tα1-GFP (B) and pDrive-hβ-actin-GFP (C) transfected OBGF400 cells. The gate for positive GFP fluorescence (M1) was derived from histogram A.

efficiency was a consequence of using the Nucleofector™ technology to penetrate the cells, the transfection ability of a plasmid (pDrive-hβ-actin-GFP) that relied on the use of an alternate, universally recognized actin promoter to express GFP was evaluated using equivalent criteria (Fig. 4C). Interestingly, the resultant percentage of GFP-positive cells was 36.6%, a value identical to that obtained for the pCI-Tα1-GFP-transfected cells. Thus, the transfection results were most likely a reflection of suboptimal procedures for neuronal cells and not due to the recognition of the Tα1 promoter by only a subset of the OBGF cell line.

3.5. Immunocytochemical analysis of OBGF400 cells

To verify the predicted neuroblast phenotype of the OBGF400 cells, they were screened for the presence of neuronally restricted protein markers. Due to a lack of suitable antibodies raised against such porcine proteins, the feasibility of using the ones recognizing counterparts from other mammalian species was tested. For this purpose, since distinct porcine neuronal and glial cell lines are not available, porcine OB tissue that contains both neural cell types was examined. In all instances, a positive reaction was noted with the OB tissue indicating specific cross-reactivities for the primary antibodies (data not shown). Moreover, at least the mouse-derived antibodies were suitable for use with OBGF400 cells since autofluorescence was not observed when an isotypic control, normal mouse IgG_1 (Fig. 5I), was used in lieu of them.

When the OBGF400 cells were treated with anti-TuJ1 antibodies (Fig. 5A), this neuron-specific class III-β tubulin protein was detected throughout their cytoplasm, a characteristic localization for lineage-restricted progenitor cells. Likewise, the neuronal precursor transcriptional regulator SOX2 also was present in the cytoplasm (Fig. 5B), another indication of their neuronal lineage-restricted neuroblast phenotype. In contrast, the neuronal progenitor marker, Nrg1, was located mainly in the nucleus of the hTERT-transduced cells (Fig. 5C). Also present was DXC (Fig. 5D), a microtubule-stabilizing protein required for migrating neuroblasts, and thus ubiquitously located in the cell body. Its punctate-staining pattern indicated that DXC has a nonhomogenous distribution in the immature OBGF400 cells.

To determine if the hTERT-transduced sensory progenitor cells were multipotent and to further confirm their neuronal lineage restriction, the OBGF400 cell line also was examined by immunocytochemical means for the presence of several glial lineage markers. Notably, neither the astrocyte-specific GFAP nor the oligodendrocyte/Schwann cell-specific CNPase and cell surface ganglioside A2B5 were detected (data not shown).

Due to the asynchronous occurrence of cellular terminal differentiation, immunostaining of mature neurons proved to be difficult. To avoid high cell density, cells only could be maintained in the chamber slides for a relatively brief period of time, and consequently, morphological change did not always occur. However, cells depicting mature neuronal morphology retained TuJ1 antigen (Fig. 5E). Moreover, actin filament dynamics due to cellular remodeling were demonstrable in the elongating neurites in immature (Fig. 5F) and the more mature (Fig. 5G) cells. These results clearly confirmed axonal and dendritic outgrowth as well as a significant decrease in cell body size during differentiation of the OBGF400 cells.

All staining patterns described above demonstrated phenotypic uniformity among the cultured, non-differentiated progenitor cells, suggesting that the OBGF400 cultures consisted of a homogeneous population. The only protein not displaying phenotypic homogeneity in the immortalized porcine neuroblasts was the cell proliferation antigen Ki-67 (Fig. 5H). This result indicated random mitotic deceleration of the cultured OBGF400 cells.

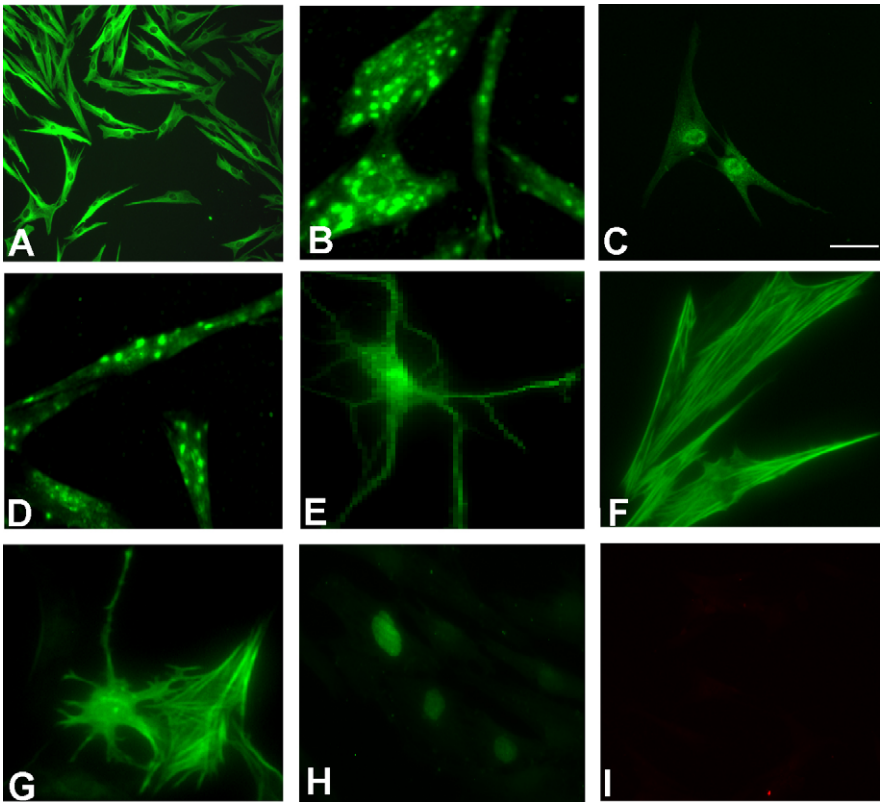

Fig. 5. Immunocytochemical characterization of OBGF400 cells. Fluorescent microscopic images of immature OBGF400 cells after the incubation with primary antibodies recognizing one of the neuron- or progenitor-specific markers TuJ1 (A, 10× objective), SOX2 (B, 40× objective), Nrg1 (C, 20× objective) or DXC (D, 20× objective) as well as the actin cytoskeleton filament (F, 40× objective) or the cell proliferation marker, Ki-67 (H, 40× objective) and subsequently exposed to FITC-labeled secondary antibody. Fluorescent microscopic images (40× objective) of phenotypically mature OBGF400 cells after the incubation with primary antibodies recognizing either TuJ1 (E) or the actin cytoskeleton filament (G). (I) The isotypic control, normal mouse IgG_1 (20× objective). Size marker in panel (C) represents 100 μm.

3.6. OBGF400 cell cycle analysis

The percentages of OBGF400 cells in the G0/G1 to G2 phases of the cell cycle were determined by using flow cytometric analysis of PI-stained cultures. A representative histogram of early subpassage cells is shown in Fig. 6. Similar profiles were obtained for late-subpassaged cells with and without G418 re-exposure (data not shown). Aneuploidy was not detected in any of the analyzed samples. The average percentage of cells in the G0/G1, S and G2 phase for early subpassage cultures was 77.9%, 17.7% and 4.4%, respectively. Comparable results were obtained for the late subpassage cultures with or without G418 re-exposure: G0/G1 (78.1% and 70.7%), S (19.4% and 21.3%) and G2 (2.2% and 8%), respectively. Most of the cells from all cultures were in G0/G1, which is in agreement with the consistent 4-day doubling time. Overall, this data indicate that the hTERT-transduced OBGF400 cells retained both a similar cell cycle balance and a normal DNA content profile (euploidy without evidence of aneuploidy) during subpassage progression.

3.7. Neuronal- and glial-specific gene expression in OBGF400 cells

Transcriptional analysis of 11 neural genes (including ones uniquely active in neuronal lineage cells, Table 1) was performed to further characterize the OBGF400 cells and to delineate their lineage restriction. Basal transcriptional patterns as existing in cells of non-neural origin were obtained using RNA from another porcine cell line (PK15) and were subsequently compared to those determined for the OBGF400 cells (Table 2).

Gene expression differences between the hTERT-immortalized neuroblasts and the PK15 cells could be grouped into three different categories based on the range of fold change (Table 2). The first group had transcriptional differences greater than 100-fold and contained the neuron-specific microtubule-associated protein 2 (MAP2) and progenitor-specific nestin genes. Their enhanced expression levels of 645.8- and 531.0-fold, respectively, in favor of OBGF400 cells were indicative of the cells' predicted neuronal progenitor lineage. Moreover, the presence of nestin in the OB-derived progenitor cells was expected based on their SVZ origin and migratory pattern via the RMS. Confirmation of these results at the protein level could not be achieved due to the lack of commercially available antibodies with sufficient reactivity against either porcine MAP2 or nestin proteins.

Further supporting an explicit neuroblast phenotype for the OBGF400 cells was the demonstration that the expression level of the third member of this group, namely the glial lineage-derived GFAP gene, was found to be 163.1-fold lower in the OBGF400 versus the PK15 cells. Considering that the latter

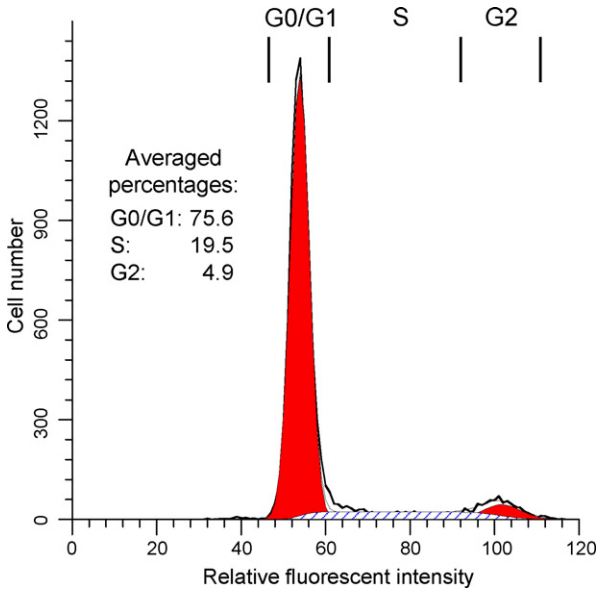

Fig. 6. Evaluation of OBGF400 cell cycle. Approximately 5×10^5 cells from two separate OBGF400 cultures each of early and late (with and without G418 re-exposure) subpassage phases were harvested on a daily basis during a 3-day period. Each sample was immediately fixed and subsequently stained with PI prior to analysis with flow cytometry. A representative histogram for an early subpassage culture in which cell number vs. relative fluorescent intensity is depicted. The range of relative fluorescent intensities corresponding to each of the three cell cycle phases (G0/G1, S and G2) is indicated. The averaged percentages from all culture data in each cycle stage are listed.

have a non-neural origin, the presence of GFAP mRNA in PK15 cells presumably reflected basal transcription. Therefore, GFAP transcript levels would be expected to be below this baseline level in the OB-derived neuroblast cell line. This difference correlated with the immunocytochemical findings, which indicated an absence of GFAP protein in OBGF400 cells (data not shown).

Table 2
Differential expression of neural lineage-specific genes in OBGF400 vs. PK15 cells

Progenitor and neuronal lineage-specific genes		Glial lineage-specific genes	
Gene ID	Fold change[a]	Gene ID	Fold change
MAP2	645.8 (+)[b]	GFAP	163.1 (−)[c]
Nestin	531.0 (+)		
ENO	24.1 (+)	CNPase	10.8 (−)
Syn1	13.4 (+)		
S100	29.6 (+)		
MAP1B	8.96 (+)	ITGAM	1.3 (−)
NTRK	Undetectable in PK15[d]	MOG	Undetectable in OBGF400[e]

[a] Gene expression was assayed by using real-time RT-PCR. Relative gene expression was quantified using the $\Delta\Delta C_t$ method. The fold change in the target gene expression, normalized to L32 gene expression, was calculated using the formula: $2^{-\Delta\Delta C_t}$.

[b] (+): fold expression higher in OBGF400 cells as compared to PK15 cells.

[c] (−): fold expression lower in OBGF400 cells as compared to PK15 cells.

[d] Expressed in OBGF400 cells (ΔC_t value = 9.1) as compared to PK15 cells (undetectable).

[e] Expressed in PK15 cells (ΔC_t value = 18.4) as compared to OBGF400 cells (undetectable).

The second category consisted of genes whose relative expression levels ranged from 10- to 30-fold in difference. This parameter for genes encoding the neuron-specific enolase (ENO), calcium-binding protein (S100) and synaptic protein (synapsin 1, Syn1) was determined to be 24.1-, 29.6- and 13.4-fold greater, respectively, in OBGF400 cells as compared to PK15 cells. In contrast, a 10.8-fold enhanced expression of oligodendrocyte/Schwann cell-specific CNPase gene was noted in PK15 cells.

The last group was composed of genes that were associated with less than 10-fold difference in expression levels. For instance, only a 1.3-fold differential in the amount of microglial-specific integrin alpha M (ITGAM, CD11b) mRNA in favor of PK15 cells was measured. This change was not considered to be significant and could be interpreted as representative of constitutive expression. Furthermore, transcripts from the other two examined genes encoding either NTRK1 (TrkA), one of three known neurotrophic tyrosine kinase receptors, or the myelin/oligodendrocyte glycoprotein (MOG), found specifically in myelinating glial cells such as oligodendrocytes and Schwann cells, were only detected in either OBGF400 or PK15 cells, respectively. The inability to measure NTRK1 or MOG gene expression in PK15 or OBGF400 cells, respectively, precluded performing a relative comparison.

3.8. Correlation between cellular senescence and neuronal maturation of OBGF400 cells

Some cultures of OBGF400 cells randomly exhibited asynchronous morphological changes consistent with terminal differentiation. Due to this observation, cellular senescence in the OBGF400 cells was assessed by histochemical detection of SA-β-Gal activity. This enabled the distinction of senescent cells versus presenescent or actively proliferating cells, and thus permitted the correlation of cellular senescence with morphological change. Based on the cellular senescence assay of three distinct cultures that were comprised of 2007 cells total, each cell was assigned to one of four categories representing the presence or absence of SA-β-Gal expression in immature (456 and 170, respectively) or mature (533 and 248, respectively) neuronal cells (mature morphological criteria were the presence of bipolar or multipolar cell processes and a more prominently defined yet smaller cell body). A significant association between neuronal maturation and SA-β-Gal activity was found ($\chi^2 = 20.45$; $p \leq 0.001$). As predicted, the negative control (CRFK cell line) failed to express a detectable amount of SA-β-Gal activity.

3.9. Association of terminal differentiation of OBGF400 cells with decreased telomerase activity and quantity of hTERT transcript levels

Some cultured hTERT-immortalized porcine neuroblasts underwent asynchronous morphology changes and seemingly matured into terminally differentiated neurons. To determine if these morphological changes correlated with a decrease in net telomerase activity, five cultures that displayed dif-

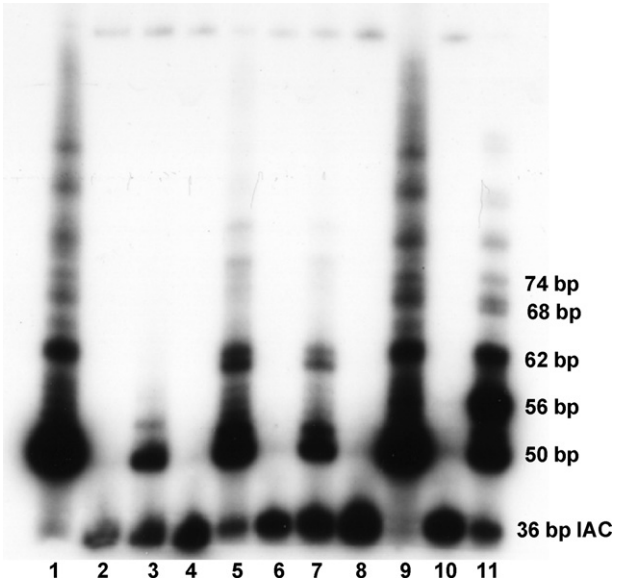

Fig. 7. Comparison of telomerase activity in OBGF400 cells retaining an immature morphology with those progressively acquiring an appearance consistent with neuronal maturation. Lysates of early-subpassaged OBGF400 (hTERT-immortalized) cells exhibiting progenitor-like immature morphology (lane 1), primary L-OB hTERT$^-$ cells (lane 3), two distinct OBGF400 early cultures with a significant degree (>50%) of morphological change indicative of maturation (lanes 5 and 7), and their respective heat-inactivated counterparts (lanes 2, 4, 6 and 8) were subjected to TRAP assays. The resultant products, separated by non-denaturing 12% polyacrylamide gel electrophoresis, were analyzed by using autoradiography. Controls consisted of a telomerase positive extract (lane 9), a primer–dimer PCR contamination control (lane 10) and a telomerase quantification control template, TSR8 (lane 11). A ladder of amplicons with 6 bp increments starting at 50 bp indicates the presence of active telomerase. Each reaction also produced a 36-bp IAC.

ferent degrees of neuronal maturation (as described above) were assayed for enzymatic activity. As terminally differentiated OBGF400 cells could not be isolated from the remaining portion of actively proliferating cells, it was impossible to determine the exact percentage of matured, post-mitotic cells in the harvested cellular lysates. However, representative results of the TRAP assay distinctively showed that telomerase activity decreased among cultures with significant terminal differentiation (Fig. 7). For example, while a value of 134 TPG/10^5 cells was established for hTERT-transduced OBGF400 cells exhibiting immature morphology (Fig. 7, lane 1), a 6.4-fold relative decrease (21 TPG/10^5 cells) was noted when primary L-OB hTERT$^-$ cells (Fig. 7, lane 3) were assayed. Interestingly, two OBGF400 cultures, in which a significant percentage (>50%) of cells exhibited a mature neuronal morphology, contained 1.9- and 3.0-fold less telomerase activity than the immature cell population as indicated by the derived values of 72 TPG/10^5 cells (Fig. 7, lane 5) and 44 TPG/10^5 cells (Fig. 7, lane 7), respectively. Although loss of telomerase activity varied substantially among the independent cellular lysates, a direct association between reduced telomerase activity and the occurrence of neuronal maturation in cultured immortalized neuroblasts was apparent.

A standardized hTERT rRT-PCR assay was utilized to determine whether a reduction of telomerase enzyme activity positively correlated with diminishing hTERT transcript levels, and thus would confirm the enzymatic assay results. For this purpose, six different, subpassaged OBGF400 cultures with varying degrees of morphological change were evaluated and a significant decrease in the amount of telomerase mRNA was found in four of them. Interestingly, the two samples that exhibited the least amount of morphological change had relatively greater telomerase transcript amounts (6.82 [±3.15]- and 4.13 [±1.68]-fold). Thus, increasing differentiation of OBGF400 cells apparently was positively associated with reduced hTERT gene expression and a corresponding loss of telomerase activity.

3.10. Permissiveness of OBGF400 cells for PrV infection and LAT gene expression

To determine the permissiveness of the OBGF400 cells for the porcine alphaherpesvirus, PrV, cultures were inoculated with a GFP-encoding mutant, PrV-Be-GFP. Approximately 90% of an OBGF400 cell population exhibited a cytopathic effect (primarily manifested as cell rounding and detachment from the vessel surface) and microscopically evident GFP production within the ensuing 16-h post-infection (data not shown). In contrast, morphological alterations and GFP production were absent in the mock-treated counterpart. Viral titrations performed on harvested culture fluids indicated that the average yield was 4.8×10^6 $TCID_{50}$/ml ($n = 4$), an amount approximately 10-fold greater than the titer of the inoculum.

In addition, temporal PrV LAT expression in the OBGF400 neuroblasts was analyzed by using rRT-PCR. Viral LAT was first detected at 4 hpi. Although its relative quantity slightly increased (1.8-fold) during the ensuing 2 h, a significant 43-fold enhancement was observed at 8 hpi. This demonstrated permissiveness of the OBGF400 cells for a PrV infection as well as their expression of LAT during a productive lytic infection. This clearly strengthens the suitability of the OBGF400 neuroblasts as a novel cell culture system for the study of neurotropic alphaherpesviruses.

4. Discussion

In this report, we describe the establishment of the first viable porcine neuroblast cell line derived from the OB. This tissue was selected as a source of neuroblasts because the adult OB is known to harbor a population of progenitor cells that display physical properties associated with differentiated neurons, yet maintain their ability to actively replicate (Coscun and Luskin, 2002). As an exception to the central dogma of neuronal maturation (Coscun and Luskin, 2002), these neuroblasts actually differentiate prior to exiting the cell cycle. However, as these cells leave the ependymal–subependymal core of the OB and migrate toward the more peripheral granule layers, their mitotic competence rapidly degrades. Whether or not the mitotic deceleration of these particular neuronal progenitor cells closely correlates with the simultaneous loss of telomerase activity through transcriptional silencing of the TERT gene remains to be determined. Regardless, we demonstrated that enabling OBGF400 cells to constitutively synthesize telomerase significantly extended their mitotic competence and that, contrary to common tenets,

these immature progenitors could be propagated in the presence of serum. Moreover, since primary non-transduced OB cells rapidly differentiated in the presence of serum and could not be cultivated beyond 6 weeks, sustained telomerase activity not only enhanced cellular proliferation capacity, but also seemingly resulted in the delay of cellular maturation. In this regard, we also showed that a loss of telomerase activity, presumably due to decreased expression of the hTERT gene, correlated with phenotypic neuronal differentiation. Interestingly, re-exposure of OBGF400 late subpassage cultures to the neomycin analog, G418, did not prevent a random, infrequent occurrence of neuronal maturation. This observation eliminated the possibility of a spontaneous reversion to a wild type, and hence $hTERT^{-}$ phenotype of some OBGF400 cells through chromosomal loss or transcriptional inactivity of the immortalization cassette.

Intrigued by the transcriptional down-regulation of telomerase expression in cultures that exhibited a significant number of mature OBGF400 neuronal cells, the identical RNA extracts were used to analyze changes in the expression of the cyclin-dependent kinase inhibitor p21 (CDKN1A), the pro-apoptotic mediators Bcl2-associated X protein (Bax) and Noxa genes (data not shown) as well as that of the proto-oncogene, c-myc. Results of the rRT-PCR assays for the presence of these particular mRNAs revealed consistent expression levels despite decreased amounts of hTERT transcripts. Consequently, altered regulation of these genes was determined not to play a role in the terminal differentiation of OBGF400 cells.

Recently identified cytokines, such as the cyclin-dependent kinase inhibitor $p19^{INK4d}$ and the bone-morphogenetic proteins, members of the transforming growth factor-β family, have been shown to play a pivotal role in cell cycle exiting and concomitant acquisition of a post-mitotic stage by OB progenitor cells (Coscun and Luskin, 2001, 2002). Although a linkage between these factors and telomerase has not yet been identified, the *in vitro* cultivation of these neuronally committed progenitor cells provides a unique opportunity to further investigate the involvement of telomerase in terminal differentiation and neuronal maturation of SVZ-derived precursors.

Characterization of the immortalized OBGF400 cells was extensively performed at the translational as well as the transcriptional level. Interpretation of these data requires consideration of the homogeneity of this novel cell line. Initially, the primary heterogeneous neural cell cultures were subjected to limiting dilutions preceding amphotrophic retroviral transduction. Furthermore, subsequent G418 resistance-based selection of hTERT-transduced neural cells yielded very few cells that maintained their capacity for mitotic expansion. Thus, the low frequency of survivors may indicate the selection of only a very specific subset of OB lineage-restricted progenitor cells. In this regard, such predicted phenotypic uniformity was established by immunocytochemical analysis. Interestingly, initial characterization at the translational level established the presence of TuJ1, one of the most commonly used neuronal markers. For instance, in immature olfactory sensory neurons of neonatal rats, TuJ1 antigen was found to localize in the neuronal cell body and processes (Lee and Pixley, 1994), a staining pattern similar to that was obtained with the OBGF400 cells (Fig. 5A). This indication of neuronal lineage commitment was supported by the detection of DXC in the cytoplasm of the OBGF400 cells. Transient expression of this protein was found to be associated with tangential migration of neuroblasts originating in the lateral ventricle of the SVZ and the RMS (Brown et al., 2003; Francis et al., 1999; Gleeson et al., 1999). Although the presence of DXC does not necessarily substantiate the exclusive commitment of the hTERT-transduced progenitor cells to the neuronal lineage, conversely, the occurrence of the progenitor markers, Nrg1 and SOX2, does not eliminate consideration of such phenotypic restriction. Neuregulins, such as Nrg1, as well as SOX2, a member of the SOXB1 transcription factor family, play a fundamental role in the survival, proliferation and differentiation of neurons and glial cells in the central and peripheral nervous systems (Graham et al., 2003; Raabe et al., 2004). In addition, SOX2 signaling has been shown to maintain neural progenitor cells of the SVZ in a proliferative state, while inhibition of SOX2 activity results in the onset of differentiation and the withdrawal from the cell cycle (Graham et al., 2003).

The only cell marker associated with phenotypic heterogeneity in the OBGF400 cells was Ki-67. This protein is strongly associated with cellular proliferation, and thus is absent in resting cells (Scholzen and Gerdes, 2000). Although Ki-67 identification in the majority of OBGF400 cells confirmed their mitotic capability, the immunolabeling intensity for Ki-67 varied extensively among individual cells. Such diversity would suggest that despite the predominant phenotypic uniformity, these immortalized OB neuroblasts are not synchronously replicating, but rather are in various stages of the cell cycle. Based on the flow cytometric cell cycle analysis, the majority of the cell population (77.4%) was in the G0/G1 phase. Accordingly, both results are most likely reflective of the established relatively slow doubling time (4 days) of the OBGF400 cells and their random exiting from the cell cycle due to neuronal maturation as supported by the SA-β-Gal cellular senescence assay. Interestingly, 37.2% of the cells with apparent immature progenitor-like morphology also expressed SA-β-Gal, suggesting that the OBGF400 neuroblasts do enter a senescent state prior to the induction of morphological changes and subsequent acquirement of a mature neuronal phenotype. It remains to be determined whether the Ki-67 immunostaining pattern inversely correlates with SA-β-Gal expression, an indicator of cellular senescence.

Presumably, true neuroblasts and their progeny mirror abundant neuronal-specific messages with simultaneous low expression of non-neuronal, glial-derived genes. Based on such conjecture, we evaluated the expression levels of 11 neural genes in the immortalized porcine OB neuroblasts and a porcine kidney epithelial cell line, and thus performed a comparative transcriptional analysis of cells with a neural versus non-neural origin. Such robust phenotypic depiction at the transcriptional level has not been previously described for any nervous system-derived, porcine lineage-committed cell type. Although relative as opposed to absolute mRNA levels were determined, the comprehensive expression pattern of the OBGF400 cells reflected an exclusive neuronal character. Specifically, the abundance of RNA originating from all analyzed genes representative of the neuronal lineage was greater in OBGF400 cells as compared

to PK15 cells. OBGF400 cells, for example, were found to have greater amounts of neuronal MAP2 and progenitor-specific nestin gene transcripts as compared to PK15 cells. Whereas the MAP2 protein, generally found in perikarya and dendritic processes of neuronal cells, functions in filopodial elaboration during neurite outgrowth (Caceres et al., 1992), the intermediate filament nestin is usually associated with dynamically dividing and migrating progenitor cells (Sahlgren et al., 2001). However, it should be noted that transcriptional analysis must be carefully considered as it merely hints at, yet does not guarantee, concomitant protein synthesis. Nevertheless, the unique porcine neural rRT-PCR analysis provided a significant and rigorous addendum to the phenotypic characterization of the OBGF400 cells and to their consideration as being neuronal precursors. Further support of this predicted phenotype was obtained by the demonstrated OBGF400 cells' recognition of the neuronal lineage-restricted Tα1 promoter (Gloster et al., 1994; Miller et al., 1987; Wang et al., 2000) in a transfected plasmid expression vector.

Attempts to induce morphological change through exposure to various differentiation inducing reagents and growth factor stimuli, including but not limited to retinoic acid, forskolin, DMSO as well as fibroblast, epidermal and nerve growth factors, have been unsuccessful to date (data not shown). The lack of a cellular response to differentiation factors (of which the vast majority are of non-porcine origin) may simply be due to the lack of appropriate receptor recognition of the non-porcine species ligands or that hTERT immortalization is altering the cellular physiology so as to change the cellular response to differentiation factors, such as by virtue of the cells not displaying the appropriate receptor. A more likely explanation may be found in a recent report regarding the human multipotent cell line, NT2, following hTERT-transduction. These cells were significantly inhibited in their ability to differentiate as compared to their non-transduced parental cells (Richardson et al., 2007). This suggests a potential influence telomerase may have on the differentiation of such progenitor cells, which in part supports our observation that hTERT mRNA and activity levels in the immortalized OBGF400 cells declined concomitantly with progressive neuronal maturation. It remains to be determined if transcriptional silencing of the ectopic hTERT over-expression will ultimately facilitate the induction of neuronal maturation and trigger mitotic senescence in the OBGF400 cells.

Not surprisingly, the OBGF400 neuroblasts were permissive for PrV infection and allowed viral LAT production. This finding concurs with our published data that utilized Northern hybridization and RT-PCR to demonstrate the presence of LAT as early as 2 hpi and up to 24 hpi in PrV-infected cultured neuronal (N1E, a mouse neuroblastoma) and non-neuronal (Mardin-Darby bovine kidney, CRFK and PK15) cell lines. Although LAT production is not considered neuron-specific (Jin and Scherba, 1999), it still will be of interest to determine whether terminal differentiation of these lineage-restricted progenitor cells will influence the permissiveness of the cells.

Our successful approach to the immortalization and identification of porcine neuroblasts presents a significant opportunity to further characterize such phenotypically restricted cells. Overall, the OBGF400 cell line provides a unique and continuous source of porcine neuronal-committed progenitors that can be used for the development of *in vitro* neuropathogenic disease models.

Acknowledgements

This material is based upon work partially supported by the Public Health Service Award No. 5R21AI61380-2 from the National Institutes of Health. The authors thank Dr. T.L. Goldberg for his advice on the statistical application for the cellular senescence assay and Dr. M.S. Kuhlenschmidt for his assistance with digital imaging. The authors also thank Drs. G.A. Iwamoto, A. Kaluha, D.L. Rock, W.M. Schnitzlein, J.L. Shisler and M.H. Vodkin for their editorial review of the manuscript.

References

Brown JP, Couillard-Despres S, Cooper-Kuhn CM, Winkler J, Aigner L, Kuhn HG. Transient expression of doublecortin during adult neurogenesis. J Comp Neurol 2003;467:1–10.

Caceres A, Mautino J, Kosik KS. Suppression of MAP2 in cultured cerebellar macroneurons inhibits minor neurite formation. Neuron 1992;9:607–18.

Coscun V, Luskin ML. The expression pattern of the cell cycle inhibitor $p19^{INK4d}$ by progenitor cells of the rat embryonic telencephalon and neonatal anterior subventricular zone. J Neurosci 2001;21:3092–103.

Coscun V, Luskin ML. Intrinsic and extrinsic regulation of the proliferation and differentiation of cells in the rostral migratory stream. J Neurosci Res 2002;69:795–802.

Counter CM, Avilion AA, Le Feuvre CE, Stewart NG, Greider CW, Harley CB, et al. Telomerase shortening associated with chromosome instability is arrested in immortal cells which express telomerase activity. EMBO J 1992;11:1921–9.

Counter CM, Hahn WC, Wei W, Dickinson-Caddle S, Beijersbergen L, Lansdorp PM, et al. Dissociation among in vitro telomerase activity, telomere maintenance, and cellular immortalization. Proc Natl Acad Sci 1998;95:14723–8.

Francis F, Koulakoff A, Boucher D, Chafey P, Schaar B, Vinet MC, et al. Doublecortin is a developmentally regulated, microtubule-associated protein expressed in migrating and differentiating neurons. Neuron 1999;23:247–56.

Gleeson J, Lin P, Flanagan L, Wals C. Doublecortin is a microtubule-associated protein and is expressed widely by migrating neurons. Neuron 1999;23:257–71.

Gloster A, Wu W, Speelman A, Weiss S, Causing C, Pozniak C, et al. The Tα1 α-tubulin promoter specifies gene expression as a function of neuronal outgrowth and regeneration in transgenic mice. J Neurosci 1994;14:7319–30.

Graham V, Khudyakov J, Ellis P, Pevny L. SOX2 functions to maintain neural progenitor identity. Neuron 2003;39:749–65.

Hierholzer JC, Killington RA. Quantitation of virus. In: Mahy BWJ, Kangro HO, editors. Virology methods manual. New York: Academic Press; 1996. p. 36.

Jin L, Scherba G. Expression of the pseudorabies virus latency-associated transcript gene during productive infection of cultured cells. J Virol 1999;73:9781–8.

Kilian A, Bowtell DD, Abud HE, Hime GR, Venter DJ, Keese PK, et al. Isolation of a candidate human telomerase catalytic subunit gene, which reveals complex splicing patterns in different cell types. Hum Mol Genet 1997;6:2011–9.

Kirschenbaum B, Nedergaard M, Preuss A, Barami K, Fraser RAR, Goldman SA. In vitro neuronal production and differentiation by precursor cells derived from the adult human forebrain. Cereb Cortex 1994;4:576–89.

Klupp BG, Hengartner CJ, Mettenleiter TC, Enquist LW. Complete, annotated sequence of the pseudorabies virus genome. J Virol 2004;78:424–40.

Lee VM, Pixley SK. Age and differentiation-related differences in neuron specific tubulin immunostaining of olfactory sensory neurons. Dev Brain Res 1994;83:209–15.

Liu Z, Martin L. Olfactory bulb core is a rich source of neural progenitor and stem cells in adult rodent and human. J Comp Neurol 2003;459:368–91.

Livak KJ, Schmittgen TD. Analysis of relative gene expression data using real-time quantitative PCR and the $2^{-\Delta\Delta C_t}$ method. Methods 2001;25:402–8.

Lois C, Alvarez-Buylla A. Long-distance neuronal migration in the adult mammalian brain. Science 1994;264:1145–8.

Mikkelsen M, Moller A, Jensen LH, Pedersen A, Harajehi JB, Pakkenberg H. MPTP-induced parkinsonism in minipigs: a behavioral, biochemical, and histological study. Neurotoxicol Teratol 1999;21:169–75.

Miller FD, Naus CC, Durand M, Bloom FE, Milner RJ. Isotypes of alpha-tubulin are differentially regulated during neuronal maturation. J Cell Biol 1987;105:3065–73.

Ormerod MG. Flow cytometry: a practical approach. 2nd ed. New York: Oxford University Press, Inc.; 1992.

Raabe TD, Deadwyler G, Varga JW, Devries GH. Localization of neuregulin isoforms and erbB receptors in myelinating glial cells. Glia 2004;45:197–207.

Reynolds BA, Weiss S. Generation of neurons and astrocytes from isolated cells of the adult mammalian central nervous system. Science 1992;255:1707–10.

Richardson RM, Nguyen B, Holt SE, Broaddus WC, Fillmore HL. Neurosci Lett 2007;421:168–72.

Roy NS, Nakano T, Keyoung HM, Windrem M, Rashbaum WK, Alonso ML, et al. Telomerase immortalization of neuronally restricted progenitor cells derived from the human fetal spinal cord. Nat Biotechnol 2004;22:297–304.

Sahlgren CM, Mikhailov A, Hellman J, Chou YH, Lendahl U, Goldman RD, Eriksson JC. Mitotic reorganization of the intermediate filament protein nestin involves phosphorylation by cdc2 kinase. J Biol Chem 2001;276:16456–63.

Scherba G, Zuckermann FA. Aujeszky's disease (pseudorabies): a natural host–virus model of human herpesviral diseases. In: Tumbleson ME, Schook LB, editors. Advances in swine in biomedical research, vol. 1. New York: Plenum Press; 1996. p. 385–94.

Scholzen T, Gerdes J. The Ki-67 protein: from the known to the unknown. J Cell Physiol 2000;182:311–22.

Smith DH, Chen XH, Nonaka M, Trojanowski JQ, Lee VMY, Saatman KE, et al. Accumulation of amyloid beta and tau and the formation of neurofilament inclusions following diffuse brain injury in the pig. J Neuropathol Exp Neurol 1999;58:982–92.

Tumbleson ME, Schook LB. Advances in swine in biomedical research, vols. 1 and 2. New York: Plenum Press; 1996.

Ulaner G, Giudice L. Developmental regulation of telomerase activity in human fetal tissues during gestation. Mol Hum Reprod 1997;3:769–73.

Wang S, Roy NS, Benraiss A, Goldman SA. Promoter-based isolation and fluorescence-activated sorting of mitotic neuronal progenitor cells from the adult mammalian ependymal/subependymal zone. Dev Neurosci 2000;22:167–76.

Wright W, Piatyszek M, Rainey W, Byrd W, Shay W. Telomerase activity in human germline and embryonic tissues and cells. Dev Genet 1996;18:173–9.